

# ULTRASOUND NEWS

August 2022



(855) 873-7666 | Log

[Store](#) [Our Solution](#) [Who We Train](#) [For Groups](#) [Company](#) [Our Clients](#) [Sup](#)

# The SonoSim Ultrasound Training Solution

Transform any computer into a remote ultrasound training platform



## Take Action

Learn how we've helped over 1,300  
and 60,000+ members

Contact Us

Full Name \*

-- Training For\* --

Title

Email \*

Phone

-- Select Country\* --

How can we help?\*



### Journals Menu

- > [Articles](#)
- > [Archive](#)
- > [Indexing](#)
- > [Aims & Scope](#)
- > [Editorial Board](#)
- > [For Authors](#)
- > [Publication Fees](#)

### Related Articles

- [Empathy Gender in Dental Students in Latin America: An Exploratory and Cross-Sectional Study](#)
- [Institutional Inefficiencies in Latin America](#)
- [The Dilemmas of Democracy in Latin America](#)

[Open Journal of Radiology](#) > Vol.11 No.4, December 2021



## Thyroid Nodule: Alpha Score 2.0 Classification for FNAB Selection, Multicentric Study in Latin America

Glenn Mena<sup>1\*</sup>, Maria Cristina Chammas<sup>2</sup>, Carlos Mario Gonzalez Vasquez<sup>3</sup>, Lylian Rocío Villagómez<sup>1</sup>, Marco Alfredo Muñoz Pico<sup>1</sup>, Patricio Alejandro Montalvo<sup>4</sup>, Santiago Mena-Bucheli<sup>5</sup>, Julio Olmedo<sup>1</sup>, Elizabeth Quintero<sup>1</sup>, Pedro Henrique de Marqui Moraes<sup>2</sup>, Osmar Cassio Saito<sup>2</sup>, Hubertino Diaz<sup>6</sup>, Denise Romero<sup>7</sup>, Gabriela Velalcazar<sup>8</sup>, Angel Ramón Sosa Fleitas<sup>9</sup>, Yamil Oliver Quevedo Ontaneda<sup>10</sup>, Victor Ricardo Chara<sup>11</sup>

<sup>1</sup>Alpha Imagen Radiología e Intervencionismo, Quito, Ecuador.

<sup>2</sup>Hospital das Clínicas Faculdade de Medicina da Universidade de São Paulo, São Paulo, Brasil.

<sup>3</sup>Hospital Pablo Tobón Uribe, Medellín, Colombia.

<sup>4</sup>Hospital del Instituto Ecuatoriano de Seguridad Social Quito Sur, Quito, Ecuador.

<sup>5</sup>Hospital San Francisco de Quito, Quito, Ecuador.

<sup>6</sup>Hospital Edgardo Rebagliati Martins, Lima, Perú.

<sup>7</sup>Hospital Carlos Andrade Marín, Quito, Ecuador.

<sup>8</sup>Hospital de Clínicas San José de San Martín, Buenos Aires, Argentina.

<sup>9</sup>Hospital Universitario de Los Andes, Mérida, Venezuela.

<sup>10</sup>Hospital de la Policía, Quito, Ecuador.

ROC					
Tested variables	Area	Deviation error <sup>a</sup>	Asymptotic significance <sup>b</sup>	95% Asymptotic confidence interval	
				Inferior limit	Superior limit
Hypoechoic	0.658	0.027	0.000	0.605	0.710
Solid consistency	0.728	0.031	0.000	0.668	0.789
Irregular borders	0.850	0.024	0.000	0.804	0.896
Microcalcifications	0.848	0.024	0.000	0.801	0.896
Shape taller than wide	0.779	0.029	0.000	0.721	0.837
Diameter = or >1.5 cm	0.500	0.046		0.411	0.589

**Table 6.** Alpha Score 2.0 ROC of predictors.

Notes: <sup>a</sup>Under the nonparametric assumption; <sup>b</sup>Null hypothesis: true area = 0.5.

Thyroid nodule: score and summation of the predictor		Benign	Low malignancy probability	Moderate malignancy probability	High malignancy probability
Hypoechoic	1				
Predominantly solid	2				
Irregular borders	2				
Shape taller than wide	2	0 - 2	3	4 - 6	7 or more
Microcalcifications	2				
Diameter equal to or greater than 1.5 cm	1				
Malignant results		1.9%	8.7%	13.6%	75.7%
Recommended action		Habitual follow up	Active vigilance	Recommended FNAB	Mandatory FNAB

**Table 7.** Alpha Score 2.0 categories compared with Bethesda and recommended score-based action.

## Abstract

**Introduction:** To perform a Latin-American multicentric study for the prediction of benign and malignant thyroid nodules using Alpha Score, and to compare it with ACR TIRADS® and Bethesda®. **Materials and Methods:** A prospective multicentric study in 10 radiological hospitals and institutions of Latin America was performed and 818 thyroid nodules were analyzed by ultrasound and classified by using both ACR TIRADS® and Alpha Score; fine-needle aspiration biopsy was performed when needed and classified with Bethesda. The relationships between predictors were analyzed by using binary logistic regression, statistical significance was defined by a p-value of 0.05, with an error margin of 4% and 95% confidence intervals. **Results:** Alpha Score 2.0 establishes five types of malignant predictors: microcalcifications, irregular borders, taller-than-wide shape, predominant solid texture and hypoechogenicity; a diameter equal to or greater than 1.5 cm adds an extra point to the final score. Resulting classification divides TNs into 4 categories: benign (1.9%), low suspicion (8.7%), mild suspicion (13.6%) and high suspicion (75.7%) of malignancy probability; sensitivity of 82%, specificity of 74%, the positive predictive value of 94%, the negative predictive value of 51%, the statistical accuracy of 81%, odds ratio of 108.89 and correlation with ACR TIRADS of 0.77 and Bethesda of 0.91. **Conclusions:** Alpha Score 2.0 has superior diagnostic accuracy and performance compared to the previously published Alpha Score and is able to classify a benign TN in a precise, safe and accurate way, avoiding unnecessary FNABs or determining the necessity of FNAB in cases of moderate to high suspicion of malignancy.

## Keywords



## Incidental Findings in POCUS: “Chance favors the prepared mind”

Sara Obeid, MD MPH<sup>1</sup>; Benjamin Galen, MD<sup>2</sup>; Trevor Jensen, MD MS<sup>3</sup>

(1) Division of Hospital Medicine at San Francisco VA Health System, Department of Medicine, University of California San Francisco, San Francisco, USA

(2) Division of Hospital Medicine, Department of Internal Medicine, Albert Einstein College of Medicine and Montefiore Medical Center

(3) Division of Hospital Medicine at UCSF Health, Department of Medicine, University of California San Francisco, San Francisco, USA

Point of Care Ultrasound (POCUS) has the potential to rapidly aide in diagnostic algorithms at the bedside, however POCUS users are often faced with the dilemma of appropriate management of incidental findings [1]. Incidental findings in POCUS are defined as any indeterminate, benign, or potentially concerning finding found unexpectedly that is not related to the patient's chief complaint [2]. Increased use of POCUS has driven the increased discovery of incidental findings, with a reported frequency between 1.6% to 26% depending on the institution, frequency of documentation, and level of experience [1,2]. While many incidental findings are benign, some are not and benefit from follow-up. This raises important concerns regarding the need for systematic, evidence-based guidelines to ensure necessary follow-up while avoiding unnecessary additional imaging, patient anxiety and increased healthcare costs [1,3].

to anticipate and manage the triage behaviors of providers who encounter a finding they are often neither looking for nor trained to evaluate. Lack of systematic, organized approaches to incidental findings with non-standard ultrasound views can lead to erroneous interpretation of acquired images and either under or over-referral to additional care. For instance, serious harm could have resulted if the aneurysm in Bouwsema and Bell's case had been noted but not acted upon rapidly. On the other hand, in a similar theoretical case of abdominal pain where large para-aortic nodes were confused with the aorta and or aortic abdominal aneurysm, unnecessary imaging could have been done, resulting in increased health care costs and patient anxiety, which is of particular importance for vulnerable and marginalized patients who experience frequent interruptions in care [1-3,7]. Furthermore, incidental findings must be communicated to the patient and

## Hickam's Dictum Incarnate: A Case of Simultaneous Left-Sided Urolithiasis and Ruptured Iliac Artery Aneurysm

Melissa Bouwsema, MD<sup>1</sup>; Colin Bell, MD<sup>2</sup>

(1) Department of Emergency Medicine, Queen's University, Kingston, ON, Canada

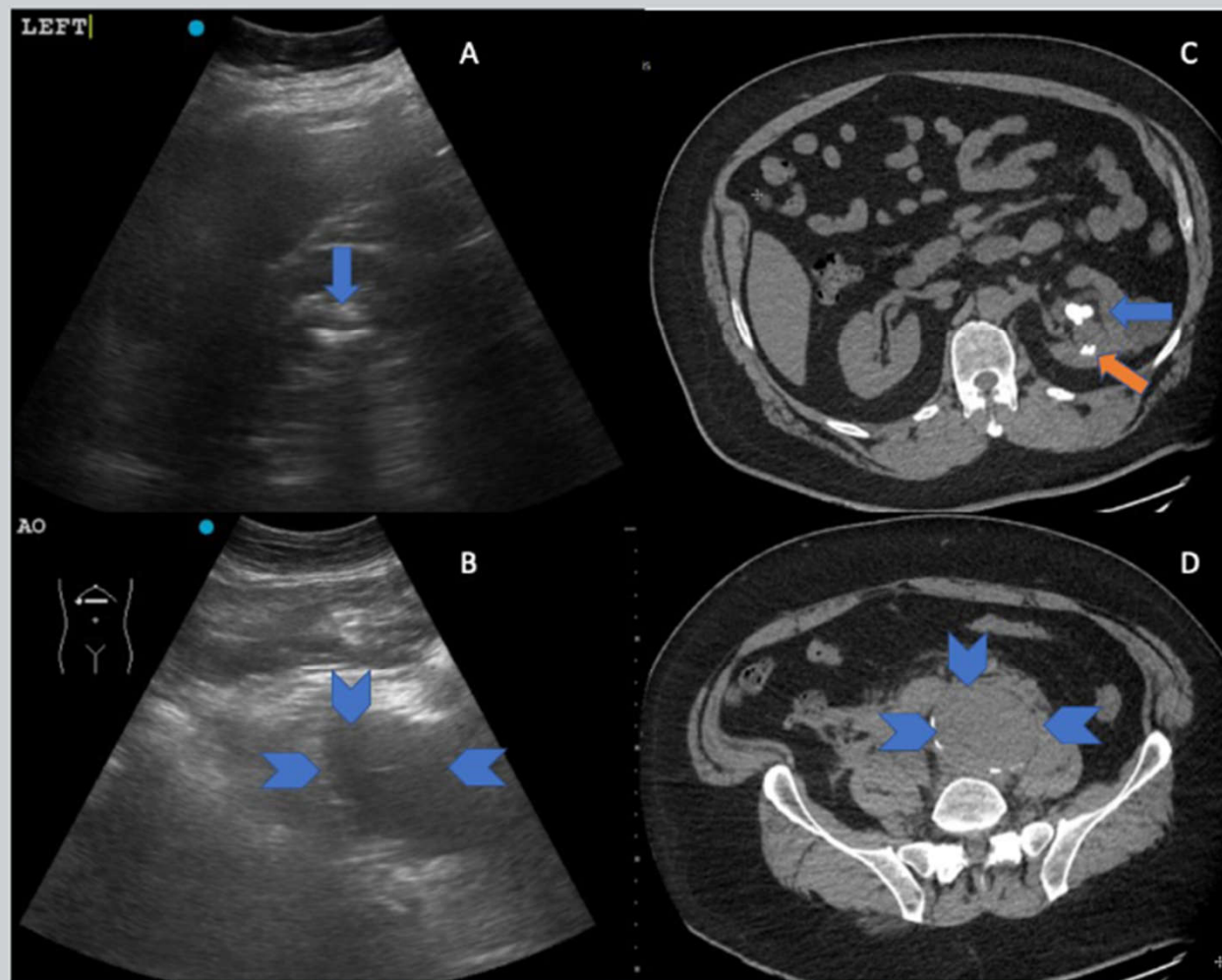
(2) Department of Emergency Medicine, University of Calgary Cumming School of Medicine, Calgary AB Canada

### Abstract

A 51-year-old man with a history of nephrolithiasis presented to the Emergency Department after a sudden onset of left-sided groin pain and syncope. At presentation, he described his pain as similar to prior renal colic episodes. At his initial assessment, point of care ultrasound (POCUS) was used, which revealed findings consistent with obstructive renal stones, as well as a substantially enlarged left iliac artery. Computed tomography (CT) imaging confirmed the comorbid diagnoses of left-sided urolithiasis and a ruptured isolated left iliac artery aneurysm. POCUS facilitated expedited definitive imaging and operative management. This case highlights the importance of performing related POCUS studies in reducing anchoring and premature closure bias.

This case highlights the importance of systematically performing related POCUS studies. Here, the operator systematically searched for AAA in spite of already having identified urolithiasis and hydronephrosis correlating with the patient's symptoms. The systematic use of POCUS, prevented the pitfall of anchoring bias and premature closure bias, both recognized as common sources of bias in diagnosis [8]. AAA is a life-threatening diagnosis, with a varied presentation, of which physical exam is particularly unreliable in detection [9].

Figure 1. A) POCUS image of left kidney with large stone in the renal pelvis (blue arrow) and hydronephrosis. B) left iliac artery (blue chevrons). C) CT image of left kidney the renal pelvis stone (blue arrow) and lower pole non-obstructing stones (orange arrow) and D) left iliac artery with aneurysm (blue chevrons).



<https://ojs.library.queensu.ca/index.php/pocus/article/view/15020/10149>



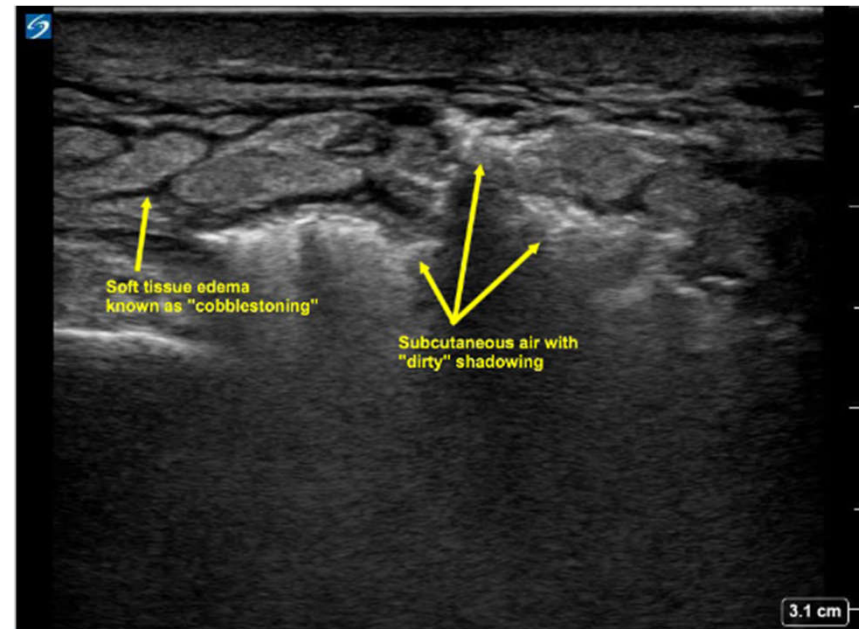
## Sonographic Crepitus, a Point-of-Care Ultrasound Finding

Brian Kohen, MD; Michael Halperin, MD MPH; Gloria Felix, MD; Trevor Dixon, MD; Michelle Montenegro, MD; Fenil Patel, MD

Albert Einstein College of Medicine, Jacobi Medical Center

### Introduction

Necrotizing fasciitis is a life-threatening polymicrobial skin and soft tissue infection that requires prompt diagnosis and treatment. Delays in diagnosis and treatment can result in an increase in morbidity and mortality [1]. Necrotizing fasciitis has historically been a clinical diagnosis. Patients with a high clinical suspicion for necrotizing fasciitis generally receive antibiotics and undergo emergent surgical debridement. In some cases, necrotizing fasciitis may be clinically difficult to differentiate from other skin and soft tissue infections such as severe cellulitis and abscesses. In such cases, POCUS may assist in diagnosis and has been shown to have a positive impact in expediting care [2,3]. Below, we describe a unique sonographic finding in a patient diagnosed with necrotizing fasciitis.



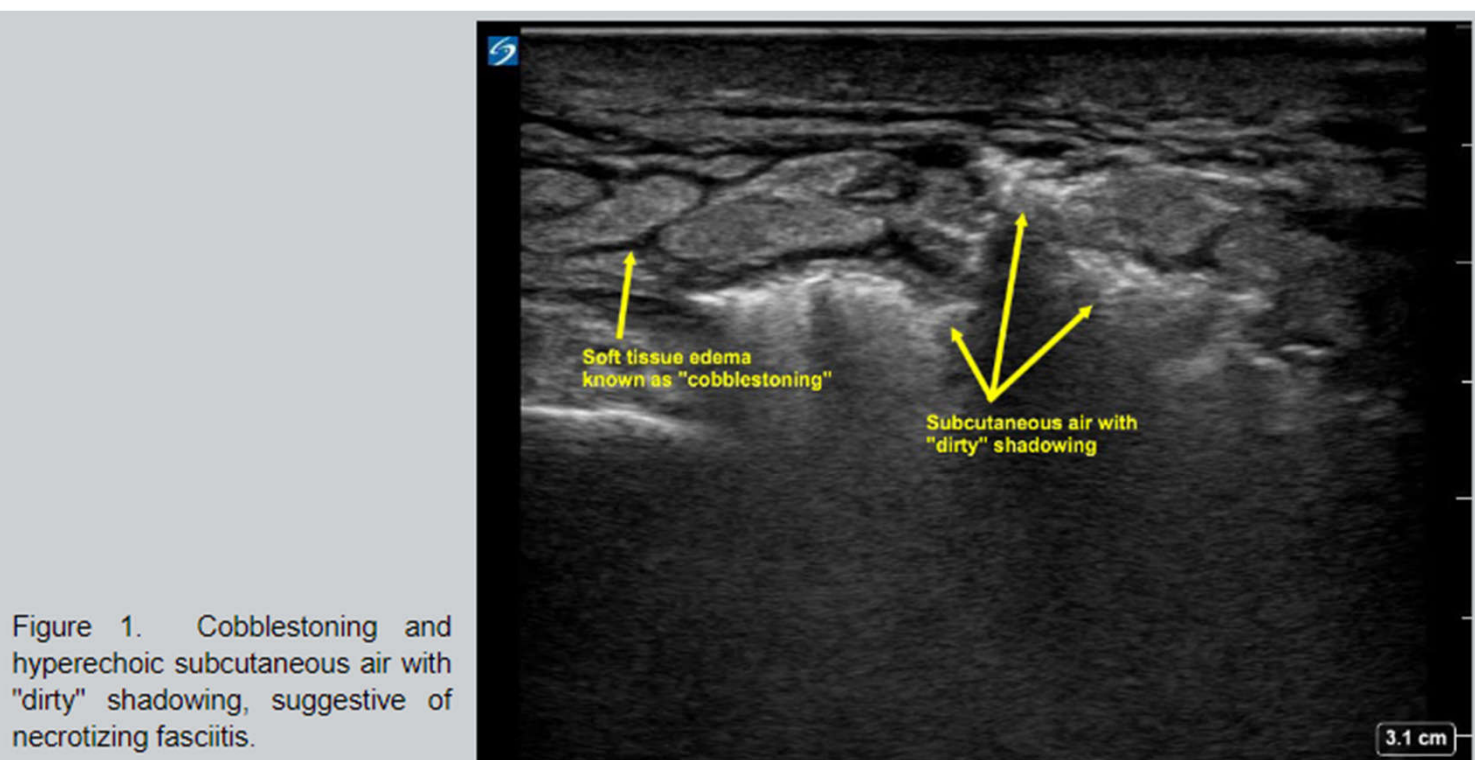


Figure 1. Cobblestoning and hyperechoic subcutaneous air with "dirty" shadowing, suggestive of necrotizing fasciitis.



Figure 2. Lateral view of a plain radiograph showing extensive subcutaneous air concerning for necrotizing fasciitis.



Review Article

## Echocardiography and Lung Ultrasound in Long COVID and Post-COVID Syndrome A Review Document of the Austrian Society of Pneumology and the Austrian Society of Ultrasound in Medicine

Martin Altersberger ✉, Georg Goliash, Mounir Khafaga, Matthias Schneider, Yerin Cho BA, Roland Winkler, Georg-Christian Funk, Thomas Binder, Gustav Huber, Ralf-Harun Zwick, Martin Genger

First published: 30 July 2022 | <https://doi.org/10.1002/jum.16068>

## Abstract

Lung ultrasound has the potential to enable standardized follow-up without radiation exposure and with lower associated costs in comparison to CT scans. It is a valuable tool to follow up on patients after a COVID-19 infection and evaluate if there is pulmonary fibrosis developing. Echocardiography, including strain imaging, is a proven tool to assess various causes of dyspnea and adds valuable information in the context of long COVID care. Including two-dimensional (2D) strain imaging, a better comprehension of myocardial damage in post-COVID syndrome can be made. Especially 2D strain imaging (left and the right ventricular strain) can provide information about prognosis.



ORIGINAL ARTICLE

Open Access



# Time course of lung ultrasound findings in patients with COVID-19 pneumonia and cardiac dysfunction

Joao Leote<sup>1\*</sup> , Tiago Judas<sup>2</sup>, Ana Luísa Broa<sup>2</sup>, Miguel Lopes<sup>3</sup>, Francisca Abecasis<sup>2</sup>, Inês Pintassilgo<sup>2</sup>, Afonso Gonçalves<sup>4</sup> and Filipe Gonzalez<sup>1</sup>

## Abstract

**Background:** Lung ultrasound (LUS) is a valuable tool to predict and monitor the COVID-19 pneumonia course. However, the influence of cardiac dysfunction (CD) on LUS findings remains to be studied. Our objective was to determine the effect of CD on LUS in hospitalized patients with COVID-19 pneumonia.

**Material and methods:** Fifty-one patients with COVID-19 pneumonia participated in the study. Focused echocardiography (FoCUS) was carried out on day 1 to separate patients into two groups depending on whether they had FoCUS signs of CD (CD+ vs CD-). LUS scores, based on the thickness of the pleural line, the B-line characteristics, and the presence or not of consolidations, were obtained three times along the patient's admission (D1, D5, D10) and compared between CD+ and CD- patients. A correlation analysis was carried out between LUS scores and the ratio of the arterial partial pressure of oxygen to the fraction of the inspired oxygen (P/F ratio).

**Results:** Twenty-two patients were CD+ and 29 patients were CD-. Among the CD+ patients, 19 were admitted to the intensive care unit (ICU), seven received invasive mechanical ventilation (IMV), and one did not survive. Among the CD- patients, 11 were admitted to the ICU, one received IMV and seven did not survive. CD+ patients showed a significantly lower P/F ratio than CD- patients. However, LUS scores showed no between-group differences, except for fewer subpleural consolidations in the upper quadrants of CD+ than on CD- patients.

**Conclusion:** In patients with COVID-19, CD contributed to a worse clinical course, but it did not induce significant changes in LUS. Our findings suggest that pathophysiological factors other than those reflected by LUS may be responsible for the differences in clinical condition between CD+ and CD- patients.

**Keywords:** LUS, Ultrasound, COVID-19, Pneumonia, Cardiac dysfunction

Act  
Go 1

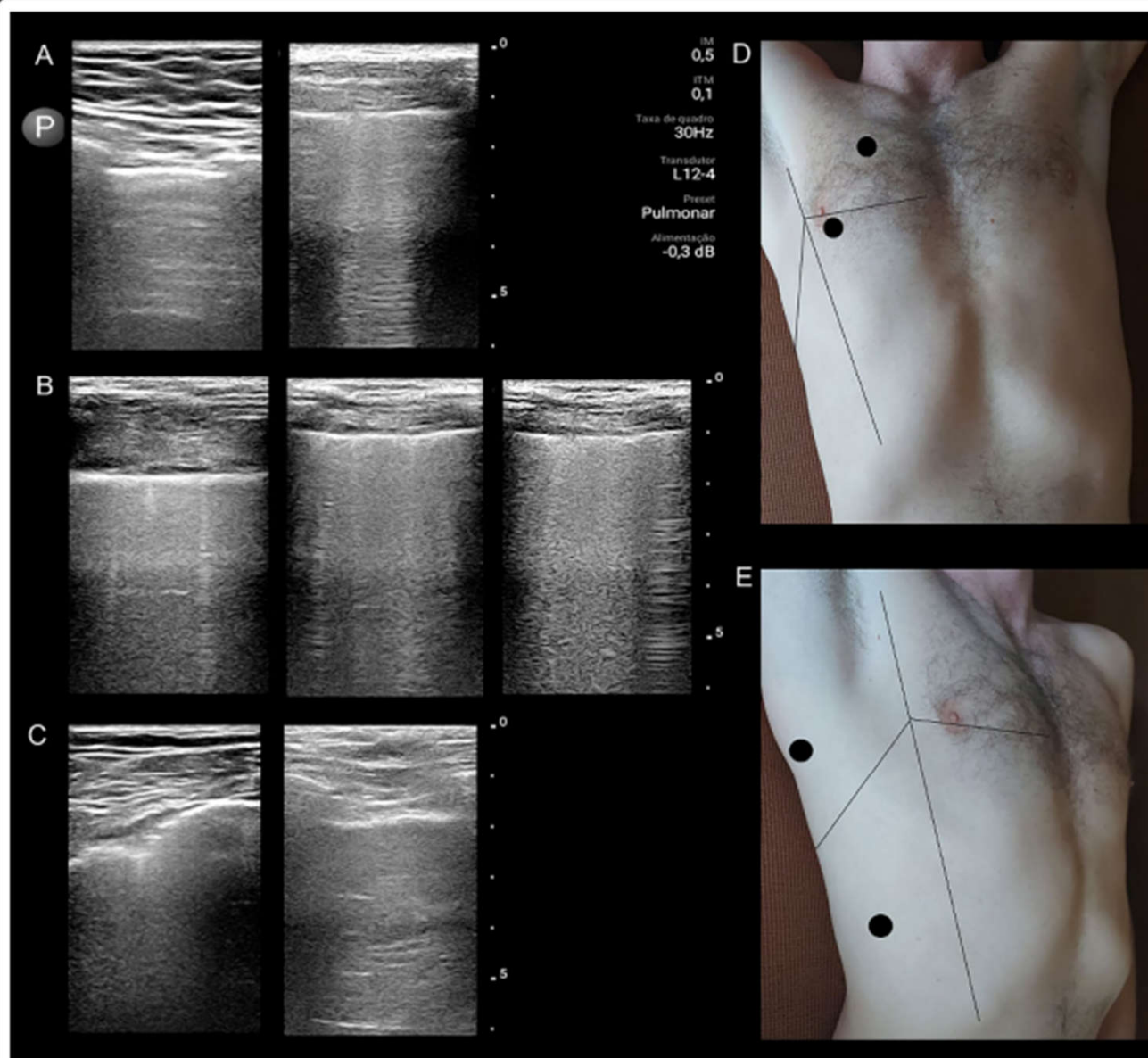


**Fig. 1** An example of lung ultrasound (LUS) findings and the procedure for calculation of LUS score. Pleura (A) was scored 1 point (left image) or 2 points (right). The B-lines presence (B) scored 1 points (left), 2 points (middle) or 3 points (right), whereas consolidations presence scored 4 points (left) or 5 points (right). The hemithorax regions evaluated are also shown including the initial probe points at each region (D and E)

Filename	Description
jum16068-sup-0001-Video1.mp4 MPEG-4 video, 13.5 MB	<b>Video S1</b> LUS and CT imaging, from the ICU to the rehabilitation—left: after acute infection with ground-glass pattern, consolidation and pleural effusion/corresponding ultrasound image of zone one, right hemithorax, lateral; right: CT and corresponding lung ultrasound 4 months later.
jum16068-sup-0002-Video2.m4v video/x-m4v, 12.8 MB	<b>Video S2</b> RV strain in a focused apical 4-ChV of the RV with normal (−23.6%) and hyperdynamic longitudinal RVF (−33.3%)
jum16068-sup-0003-Video3.m4v video/x-m4v, 13 MB	<b>Video S3</b> Strain imaging of the LV in post-COVID-19 patients with reduction in regional basal strain with normal GLS (GLS range −19.2% to −22.1%)
jum16068-sup-0004-Video4.m4v video/x-m4v, 9.6 MB	<b>Video S4</b> Strain imaging in a post-COVID-19 patient after an acute coronary syndrome with a reduction in GLS (−14.1%) and regional strain




ORIGINAL ARTICLE

Open Access



# Prehospital portable ultrasound for safe and accurate prehospital needle thoracostomy: a pilot educational study

Zachary E. Dewar<sup>1\*</sup> , Stephanie Ko<sup>1,2</sup>, Cameron Rogers<sup>3</sup>, Alexis Oropallo<sup>1</sup>, Andrew Augustine<sup>1</sup>, Ankitha Pamula<sup>1</sup> and Christopher L. Berry<sup>1</sup> 

## Abstract

**Background:** Simulated needle thoracostomy (NT) using ultrasound may reduce potential injury, increase accuracy, and be as rapid to perform as the traditional landmark technique following a brief educational session. Our objective was to determine if the use of an educational session demonstrating the use of handheld ultrasound to Emergency Medical Services (EMS) staff to facilitate NT was both feasible, and an effective way of increasing the safety and efficacy of this procedure for rural EMS providers.

**Methods:** A pre/post-educational intervention on a convenience sample of rural North American EMS paramedics and nurses. Measurement of location and estimated depth of placement of needle thoracostomy with traditional landmark technique was completed and then repeated using handheld ultrasound following a training session on thoracic ultrasound and correct placement of NT.

**Results:** A total of 30 EMS practitioners participated. Seven were female (23.3%). There was a higher frequency of dangerous structures underlying the chosen location with the landmark technique 9/60 (15%) compared to the ultrasound technique 1/60 (1.7%) ( $p = 0.08$ ). Mean time-to-site-selection for the landmark technique was shorter than the ultrasound technique at 10.7 s (range 3.35–45 s) vs. 19.9 s (range 7.8–50 s), respectively ( $p < 0.001$ ). There was a lower proportion of correct location selection for the landmark technique 40/60 (66.7%) when compared to the ultrasound technique 51/60 (85%) ( $p = 0.019$ ). With ultrasound, there was less variance between the estimated and measured depth of the pleural space with a mean difference of 0.033 cm (range 0–0.5 cm) when ultrasound was used as compared to a mean difference of 1.0375 cm (range 0–6 cm) for the landmark technique (95% CI for the difference 0.73–1.27 cm;  $p < 0.001$ ).

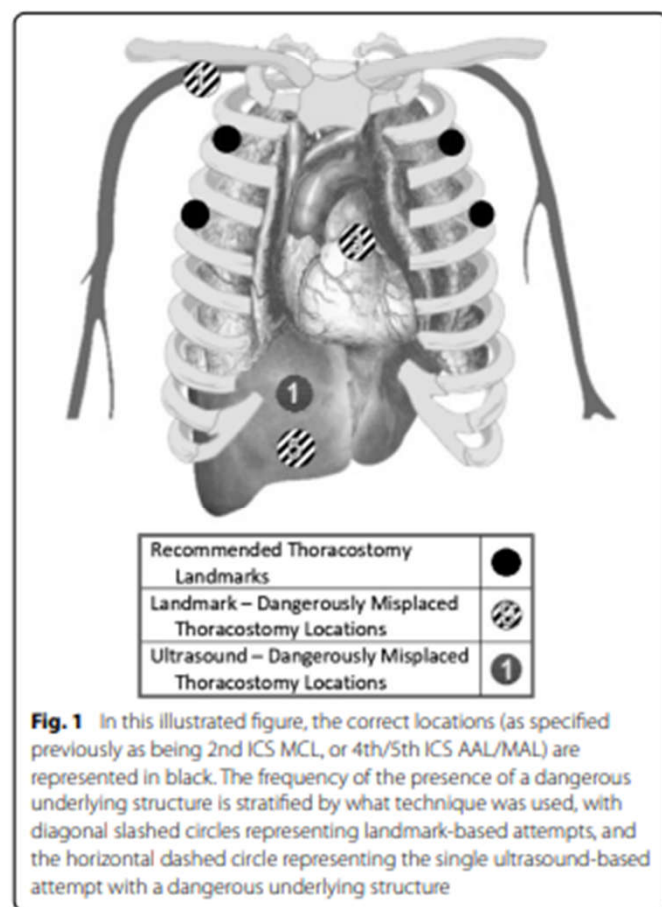
**Conclusions:** Teaching ultrasound NT was feasible in our cohort. While time-to-site-selection for ultrasound-guided NT took longer than the landmark technique, it increased safe and accurate simulated NT placement with fewer identified potential iatrogenic injuries.



**Table 2** Outcome measurements by the use of ultrasound as compared to the landmark technique

	Ultrasound (n = 60)	Landmark (n=60)	p
Dangerous underlying structure	1/60 (1.7%)	9/60 (15%)	0.008
Time to completion, s			
Mean (SD)	19.9 (10.6)	10.7 (7.1)	< 0.001
Median (range)	17 (7.8–50)	9.21 (3.35–45)	
Correct placement*	51/60 (85%)	40/60 (66.7%)	0.019

\*Defined as in the correct interspace and midline location specified for the attempt



---

# Ultrasound imaging for inguinal hernia: a pictorial review

Wei-Ting Wu<sup>1,2</sup>, Ke-Vin Chang<sup>1,2,3</sup>, Chih-Peng Lin<sup>4</sup>, Chi-Chuan Yeh<sup>5,6</sup>, Levent Özçakar<sup>7</sup>

<sup>1</sup>Department of Physical Medicine and Rehabilitation, National Taiwan University Hospital, Bei-Hu Branch, Taipei; <sup>2</sup>Department of Physical Medicine and Rehabilitation, National Taiwan University College of Medicine, Taipei; <sup>3</sup>Center for Regional Anesthesia and Pain Medicine, Wang-Fang Hospital, Taipei Medical University, Taipei; Departments of <sup>4</sup>Anesthesiology, <sup>5</sup>Medical Education, and <sup>6</sup>Surgery, National Taiwan University Hospital, College of Medicine, National Taiwan University, Taipei, Taiwan; <sup>7</sup>Department of Physical and Rehabilitation Medicine, Hacettepe University Medical School, Ankara, Turkey

Inguinal hernia is the most prevalent type of abdominal wall hernia. Indirect inguinal hernia is twice as common as direct inguinal hernia. Computed tomography and magnetic resonance imaging can be used to evaluate inguinal hernia, but these modalities are greatly limited by their cost and availability. Ultrasonography has emerged as the most convenient imaging tool for diagnosing inguinal hernia due to its advantages, such as portability and absence of radiation. The present pictorial review presents an overview on the use of ultrasonography in the evaluation of inguinal hernia with a particular emphasis on the regional anatomy, relevant scanning tips, identification of subtypes, postoperative follow-up, and diagnosis of pathologies mimicking inguinal hernia.

**Keywords:** Inguinal hernia; Ultrasonography; Groin; Hernia repair; Hernia recurrence

**Key points:** The inferior epigastric artery is the most important landmark for differentiating between indirect and direct inguinal hernias. Dynamic ultrasound imaging combined with postural changes and the Valsalva maneuver is helpful for symptom reproduction. In patients undergoing hernia repair surgery, ultrasound imaging is helpful for detecting postoperative complications and recurrence of hernia.

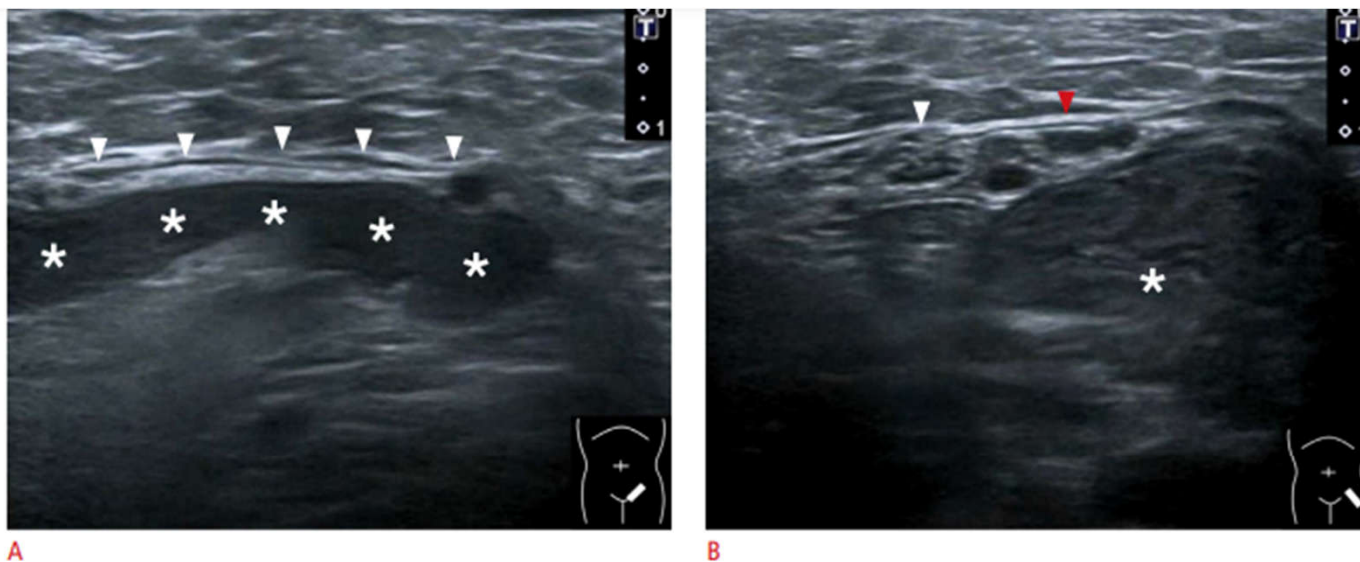


**Fig. 3.** Ultrasonography in a man with indirect inguinal hernia.

**A.** The transducer was placed in the long-axis view to visualize the hernia sac, the inside of which contained peritoneal fat and bowels (asterisks in **A** and **B**). **B.** The transducer was placed in the short-axis view to visualize the hernia sac. White arrowheads and red arrowhead indicate spermatic cord and testicular vessel, respectively.

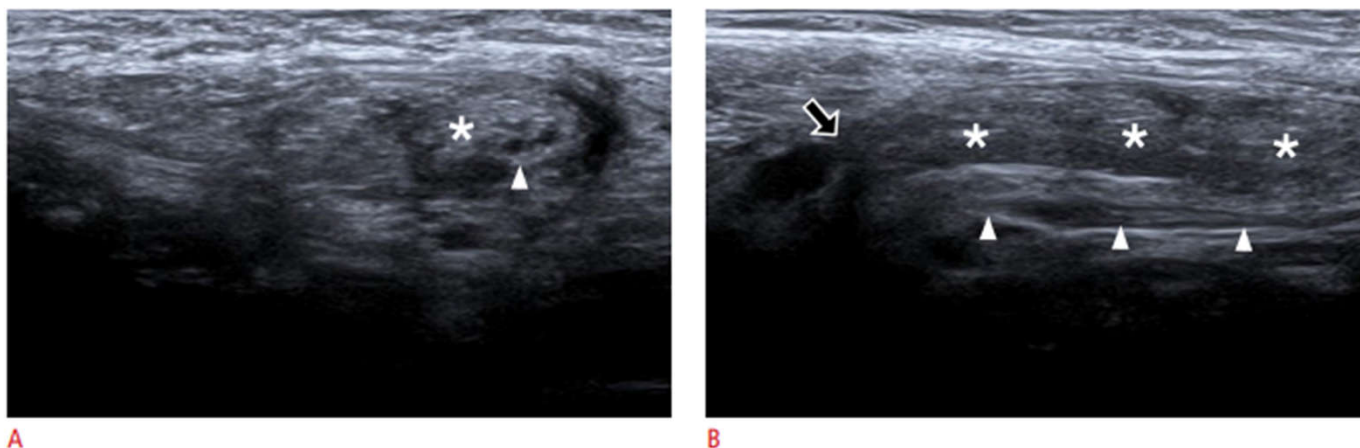


**Fig. 4.** Ultrasonography in another man with indirect inguinal hernia.

**A.** The transducer was placed in the short-axis view to visualize the hernia sac, the inside of which contained peritoneal fat and bowels (asterisks in **A** and **B**). **B.** The transducer was placed in the long-axis view to visualize the hernia sac. The deep inguinal ring (black arrow) could be visualized at the cranial side of the hernia sac. White arrowheads indicate spermatic cord.



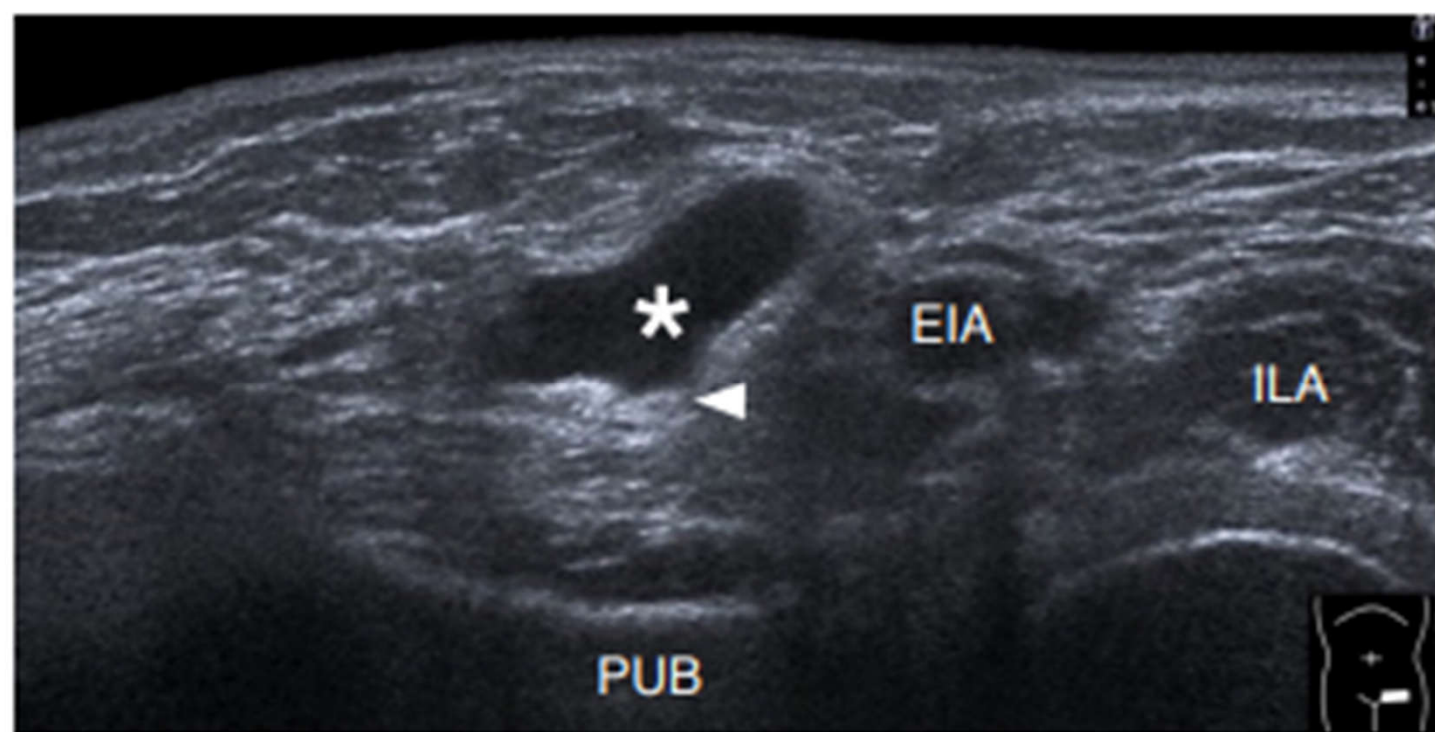
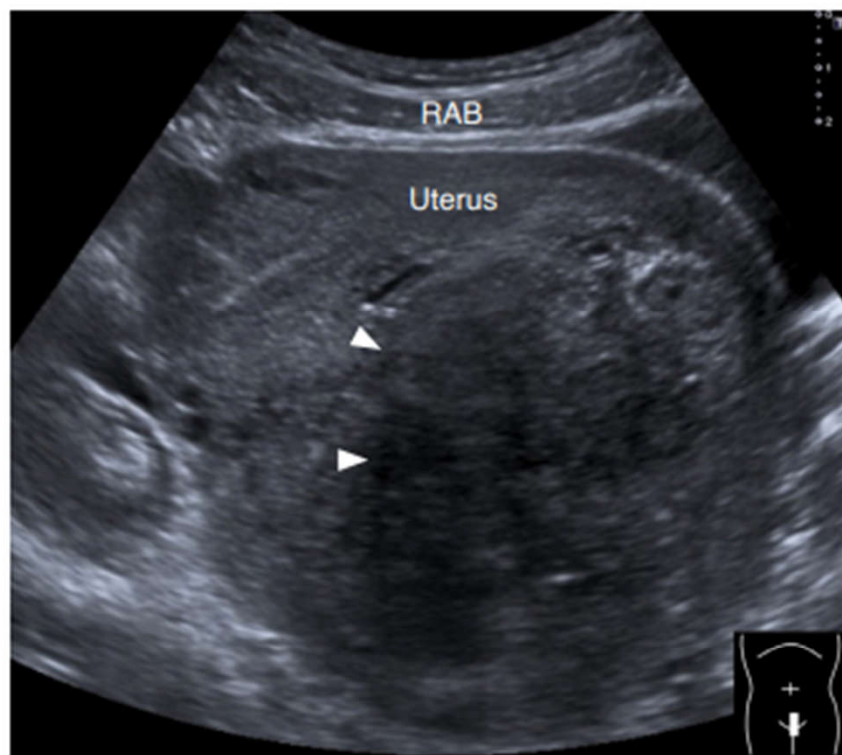
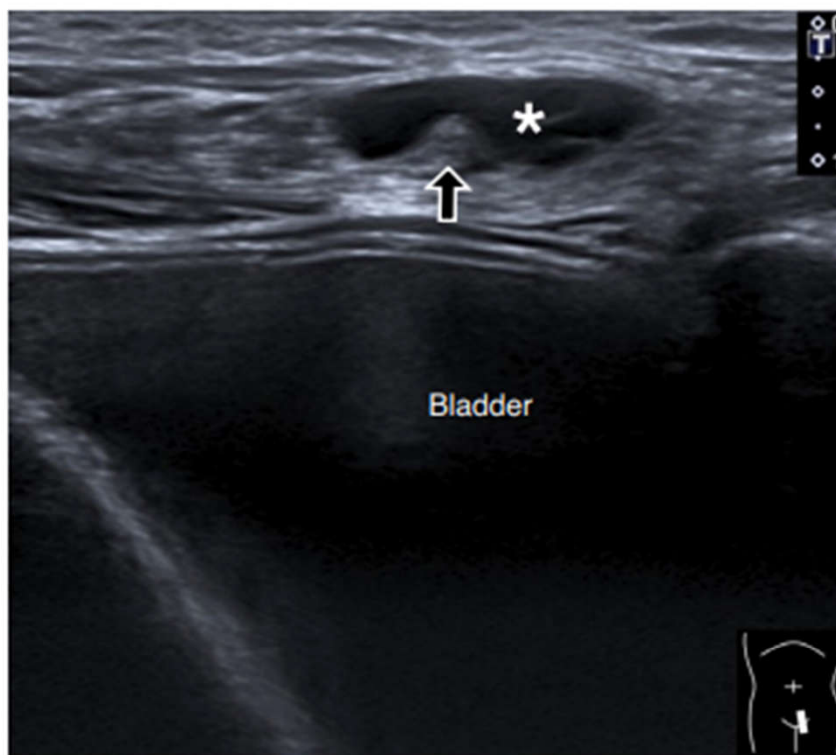


**Fig. 7.** Ultrasonography of bladder hernia. Ultrasonography reveals an anechoic compressible cyst (asterisk) beside the external iliac artery (EIA), with a tract extending to the bladder (arrowhead). ILA, iliacus muscle; PUB, pubic bone.





**A**



**B**

**Fig. 8.** Ultrasonography of fluid accumulation inside the canal of Nuck in a woman.

**A.** Ultrasonography reveals a very large myoma (arrowheads). **B.** Ultrasonography demonstrates an accidental finding of fluid accumulation (asterisk) inside the canal of Nuck. Black arrow indicates round ligament. RAB, rectus abdominis muscle.

Act  
Go t

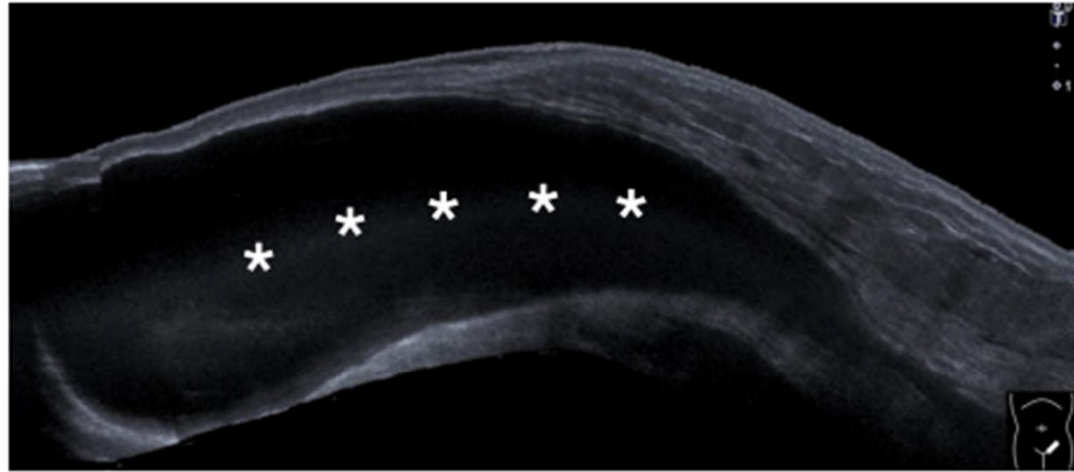
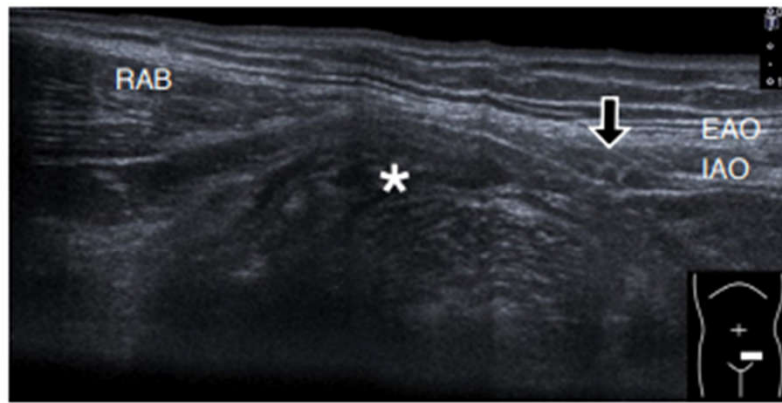
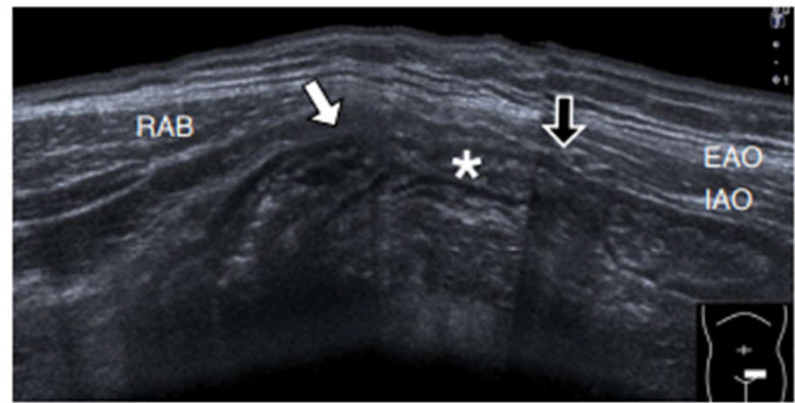


**Fig. 9.** Ultrasonography of a very large hydrocele in a man. Ultrasonography reveals a very large anechoic cyst (asterisks) extending thorough the inguinal canal.



**A**



**B**

**Fig. 10.** Ultrasonography in a patient with direct inguinal hernia.

**A.** Ultrasonography was obtained over Hesselbach's triangle during the supine resting position. **B.** Ultrasonography was obtained over Hesselbach's triangle during the Valsalva maneuver, showing the bowel contents protruding toward the abdominal wall. EAO, external abdominal oblique muscle; IAO, internal abdominal oblique muscle; RAB, rectus abdominis muscle. Black arrows, inferior epigastric artery; asterisks, herniation content (bowels); white arrow, indicating protrusion of the underlying bowels.

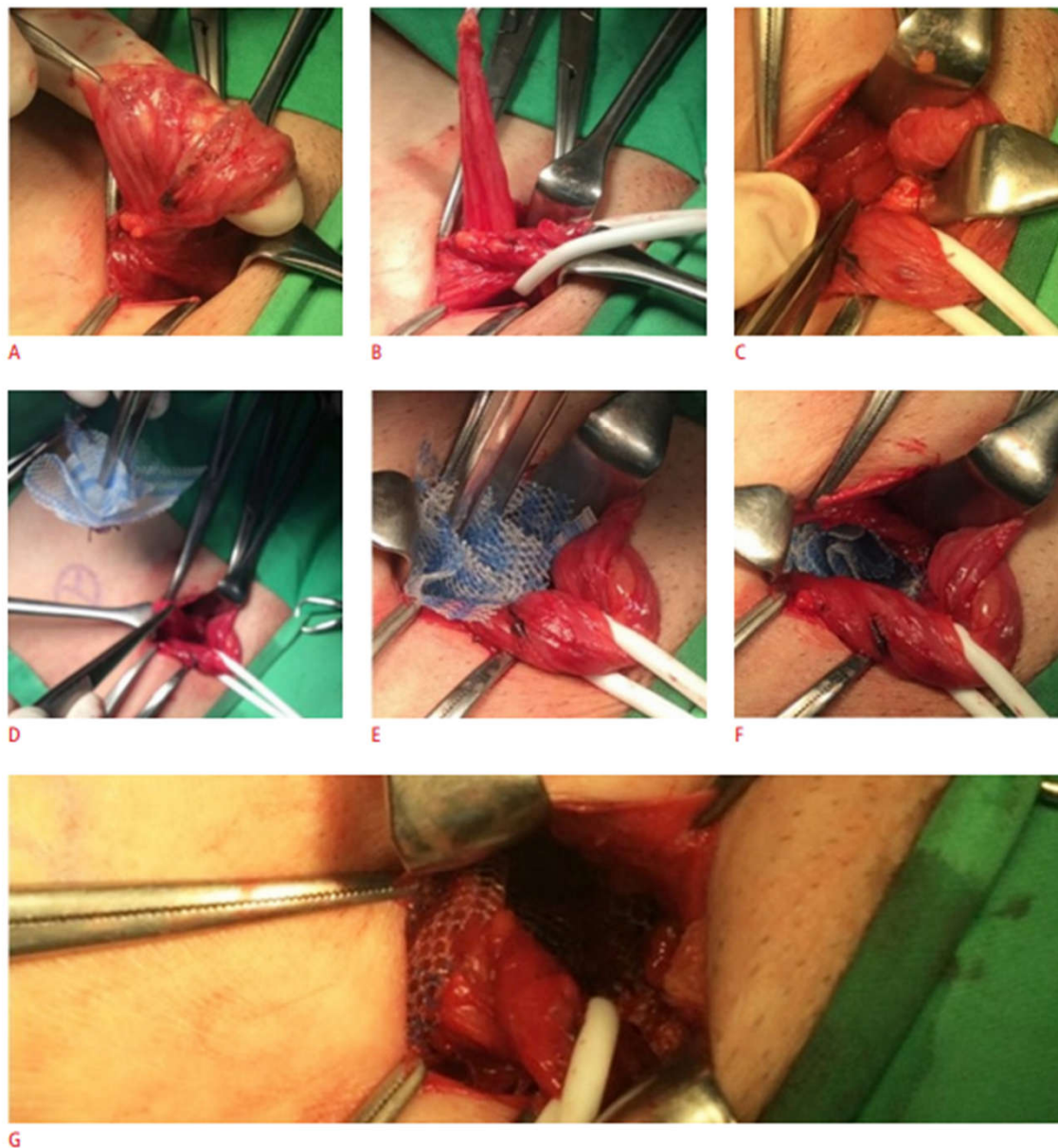
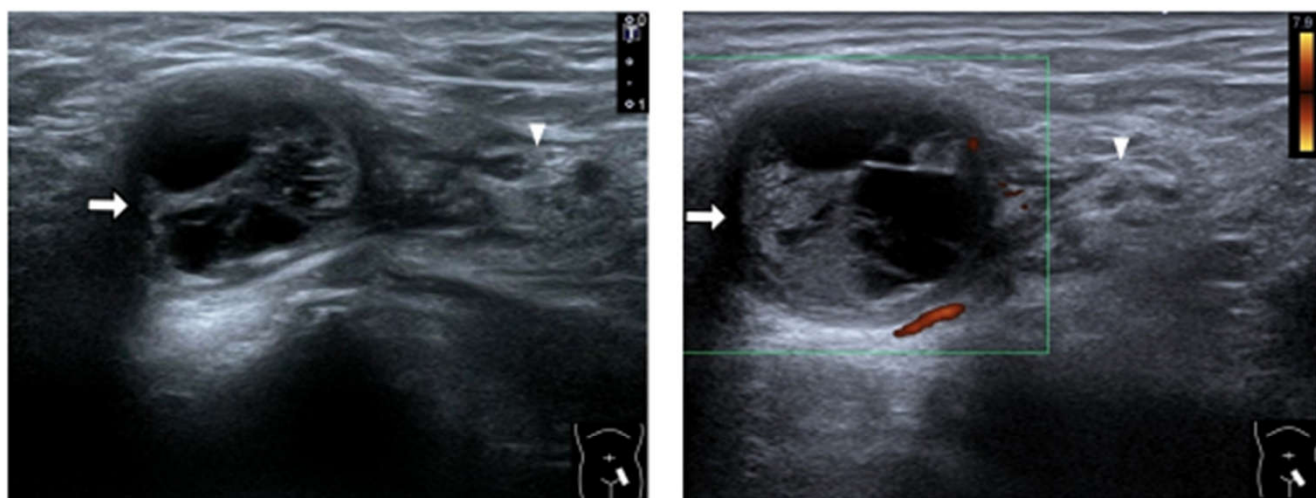


**Fig. 11.** The mesh plug method for hernia repair in a male patient with indirect inguinal hernia. **A.** Initially, the hernia sac was identified. **B.** The hernia sac was separated from the spermatic cord. **C.** The hernia sac was reduced back to the abdominal cavity. **D.** A cone-shaped mesh was prepared for plugging. **E.** The mesh was plugged through the deep inguinal ring. **F.** After being plugged, the mesh was fixed on the abdominal wall. **G.** Finally, a patch of mesh was placed to enforce the posterior wall. The series of figures are reprinted from Huang CS (2021). In: Yeh CC, ed. NTU surgery core course [14], with permission of National Taiwan University College of Medicine.



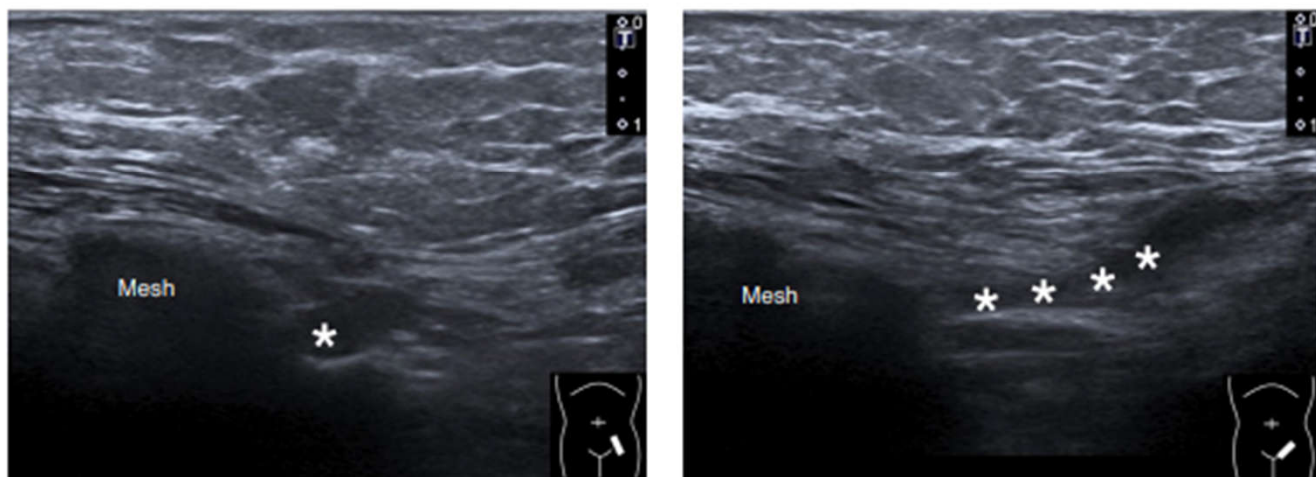


A

B

**Fig. 12.** Ultrasonography of a hematoma after a hernia repair.

**A.** Ultrasonography was obtained over the inguinal region using the B mode, revealing a circular hypoechoic structure with multiple intralesional septa. **B.** Ultrasonography was obtained over the inguinal region using the power Doppler imaging, showing an increase in peripheral vascularity of the lesion. White arrows, hematoma; white arrowheads, spermatic cord.



A

B

**Fig. 13.** Ultrasonography of recurrence after surgical repair for indirect inguinal hernia.

**A.** Ultrasonography was obtained in the short-axis view of the inguinal canal. **B.** Ultrasonography was obtained in the long-axis view of the inguinal canal. Asterisks indicate hernia sac with peritoneal fat.



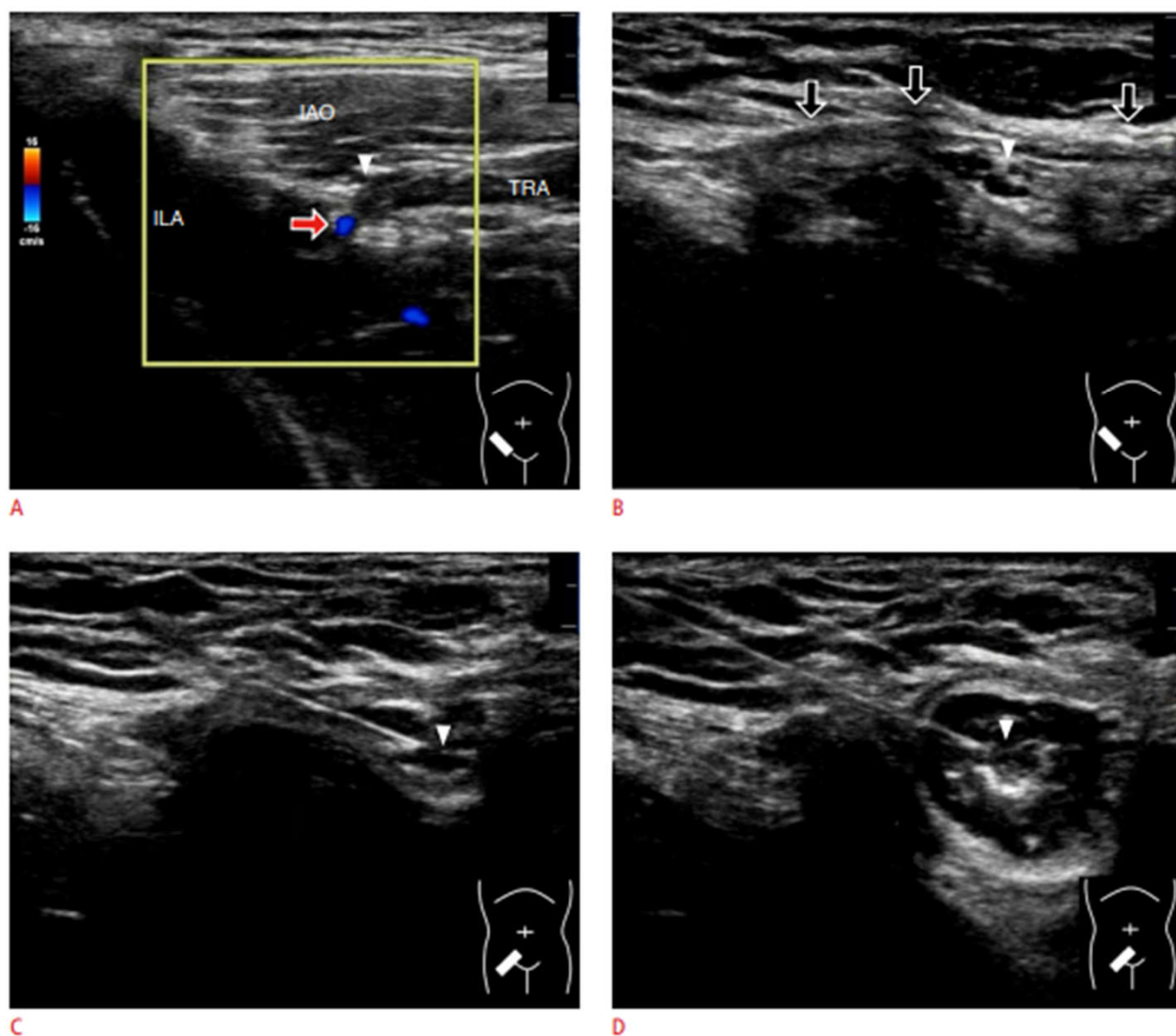
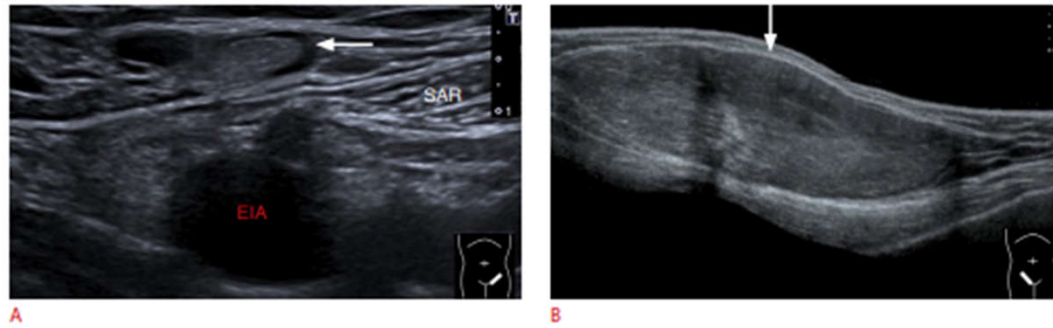


**Fig. 16.** Demonstration of ultrasound-guided ilioinguinal nerve block in a man.

**A.** The ilioinguinal nerve (arrowhead in A–D) was located between the internal abdominal oblique (IAO) and transverse abdominis (TRA) muscles at the level of the iliac crest. Red arrow indicates deep iliac circumflex artery. **B.** The transducer was moved medially to visualize the nerve emerging toward the undersurface of the aponeurosis (black arrows) of the external abdominal oblique muscle. **C.** The needle was inserted from the lateral aspect of the inguinal area to target the nerve. **D.** The injectate was distributed surrounding the nerve. ILA, iliacus muscle.

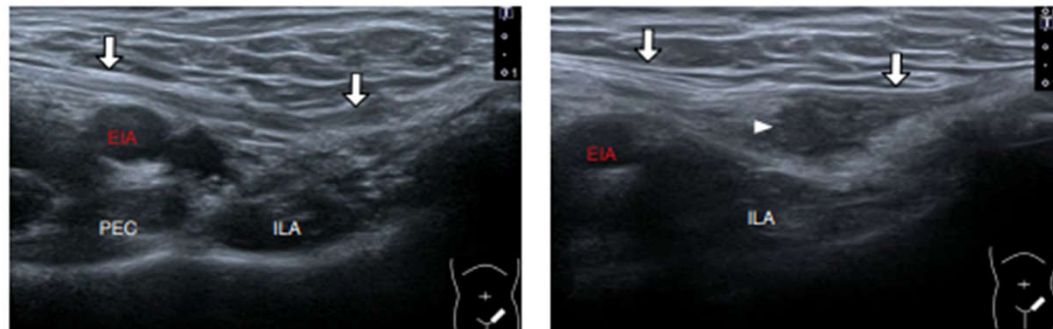


A

B

**Fig. 17.** Ultrasonography of common pathologies mimicking inguinal hernia.

**A.** Ultrasonography reveals lymphadenopathy (arrow) at the inguinal region. **B.** Ultrasonography shows a very large lipoma (arrow) at the inguinal region. EIA, external iliac artery; SAR, sartorius muscle.



A

B

**Fig. 18.** Ultrasonography of endometriosis in the inguinal region in a woman.

**A.** The transducer was placed along the inguinal ligament (white arrows in A and B) in its long axis. **B.** Ectopic endometrium (arrowhead) was shown by relocating the transducer more caudally. EIA, external iliac artery; ILA, iliacus muscle; PEC, pectineus muscle.

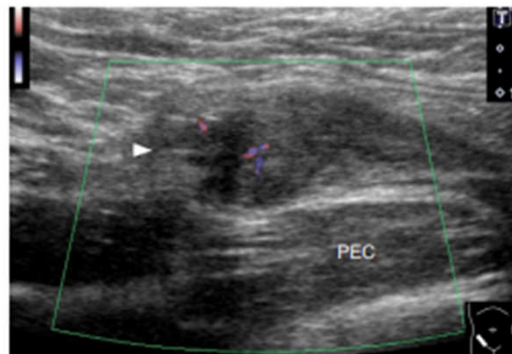


**Fig. 19.** Power Doppler ultrasonography of ectopic endometrium in a woman. The power Doppler ultrasonography reveals increased vascularity inside the ectopic endometrium (arrowhead). PEC, pectineus muscle.

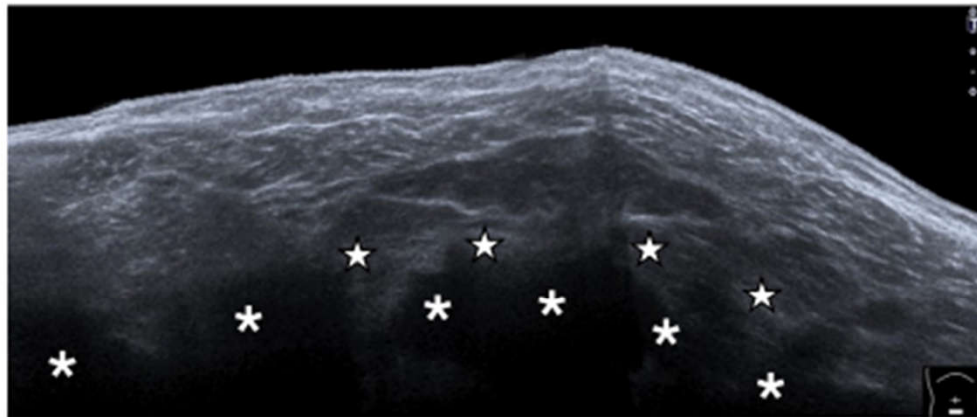
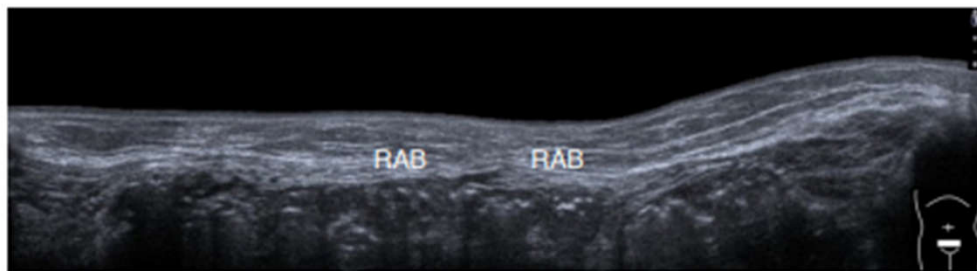


**Fig. 20.** Ultrasonography of ascites. Ultrasonography reveals anechoic homogenous fluid collection with posterior enhancement caused by ascites (asterisks) in the panoramic view. Stars, peritoneal fat.



A




B

**Fig. 21.** Ultrasonography of the protruding abdominal wall in a patient with sarcopenia. **A.** Ultrasonography was obtained in the supine resting position. **B.** The lower abdominal wall protruded forward (arrow) in the standing position. RAB, rectus abdominis muscle.



# Stiffness of Muscles and Tendons of the Lower Limb of Professional and Semiprofessional Athletes Using Shear Wave Elastography

Claudia Romer, MD, MPH , Julia Czupajlo, Enrico Zessin, Thomas Fischer, MD, Bernd Wolfarth, MD, Markus H. Lerchbaumer, MD

Received April 19, 2022, from the Department of Sports Medicine, Charité—Universitätsmedizin Berlin, Humboldt-Universität zu Berlin, Berlin, Germany (C.R., J.C., E.Z.); and Department of Radiology, Charité—Universitätsmedizin Berlin, Humboldt-Universität zu Berlin, Berlin, Germany (T.F., B.W., M.H.L.). Manuscript accepted for publication June 29, 2022.

Address correspondence to Claudia Romer, MD, MPH, Department of Sports Medicine, Charité—Universitätsmedizin Berlin, Campus Charité Mitte, Charitéplatz 1, 10117 Berlin, Germany.

E-mail: [claudia.romer@charite.de](mailto:claudia.romer@charite.de)

## Abbreviations

**Objective**—Shear wave elastography (SWE) allows assessment of muscle and tendon stiffness and can be used to diagnose soft tissue pathologies such as tendinopathies. In sports medicine, SWE may have the potential to uncover structural changes early on before they lead to functional impairment. To systematically analyze possible differences in tendon and muscle stiffness of the lower limb between professional (PG) and semiprofessional female athletes (SG) using SWE and to compile reference values for developing preventive medicine approaches for professional athletes.

**Methods**—Standardized SWE of both lower limb tendons and muscles (Achilles tendon [AT], soleus muscle insertion [SM], patellar tendon [PT], quadriceps tendon [QT], vastus medialis muscle [VM]) in the longitudinal plane was performed with the tendons in relaxed position in 24 healthy professional female athletes (PG) in comparison with 24 healthy semiprofessional female athletes (SG).

**Results**—Median tendon and muscle stiffness was significantly higher in professional athletes (AT:PG, 11.12 m/s vs SG, 7.33 m/s,  $P < .001$ ; SM: 1.77 m/s vs 1.14 m/s,  $P < .001$ ; VM: 1.63 m/s vs 0.87 m/s,  $P < .001$ ; QT: 3.31 m/s vs 2.61 m/s,  $P < .05$ ). There was no significant difference in patellar tendon stiffness between PG and SG (PT: 2.57 m/s vs 3.21,  $P = .25$ ).

**Conclusion**—Professional female athletes have higher stiffness values than semiprofessional female athletes in lower limb muscles and tendons, except for the patellar tendon. Knowledge of such differences is necessary for diagnosing tendinopathy and injuries. Musculoskeletal SWE could offer great benefits in sports medicine as well as in rehabilitation and preventive medicine.



